

# Dynamic Mechanical and Impact Properties of PP/SEBS Blend

A. K. GUPTA and S. N. PURWAR *Centre for Materials Science and  
Technology, Indian Institute of Technology, New Delhi-110 016, India*

## Synopsis

Studies on impact behaviour of the blend of isotactic polypropylene (PP) with styrene-*b*-ethylene-co-butylene-*b*-styrene triblock copolymer (SEBS) in the composition range 0–25 wt % SEBS at three temperatures, viz., ambient, –30°C, and –190°C, are presented. Dynamic mechanical properties on a torsion pendulum in the temperature range –100–100°C are also studied for this blend at various compositions. Scanning electron microscopic studies of the impact-fractured surfaces are presented to illustrate the differences in the mode of fracture at the three temperatures of impact tests. Choice of the three temperatures for impact tests was such that the effect of shear yielding mechanism of toughening of PP at ambient temperature remains suppressed at –30°C, whereas at the lowest temperature (i.e., –190°C) the elastomeric role of the inclusion SEBS is suppressed. The observed considerably large difference in impact toughening at ambient temperature and at –30°C seems not entirely accountable by the prevalence of shear yielding or crazing mechanisms in the respective temperature regions. A third mechanism, viz., viscoelastic energy dissipation, is invoked to account for the observed large difference of impact toughening at these two upper temperatures. Correlation of peak area of dynamic mechanical loss peaks occurring below the impact test temperature with the impact strength is also shown. This suggests greater significance of viscoelastic energy dissipation mechanism in the toughening of this blend at ambient temperature than at –30°C.

## INTRODUCTION

The possibility of tailoring the properties of polypropylene (PP) by incorporation of adequate impact modifiers, explored by many authors<sup>1–15</sup> in recent years, resulted in an everincreasing use of impact modified PP. Various elastomers have been used for modification of impact and other properties of PP; such as the copolymers ethylene-propylene (EPM) and ethylene-propylene-diene (EPDM),<sup>1–12</sup> hydrogenated polybutadiene,<sup>13</sup> styrene-butadiene rubber,<sup>14</sup> acrylonitrile-butadiene-styrene terpolymer,<sup>15</sup> etc. A recently commercialised thermoplastic elastomer, viz. styrene-*b*-ethylene-co-butylene-*b*-styrene triblock copolymer (SEBS) (trade name Kraton G-1652), seems an interesting material to be explored for its impact modifying role on PP. Studies on various properties of PP/SEBS blend, reported recently,<sup>16–18</sup> have shown some advantages of blending SEBS with PP thus generating interest in the exploration of impact behavior of this blend.

We present in this paper a study of impact behavior of PP/SEBS blend in the composition range 0–25 wt % SEBS content. Notched Izod impact strength and scanning electron microscopy of impact fractured surfaces were done at three temperatures chosen so as to represent the behavior in the three states of the blend: (i) rubbery inclusions in flexible matrix, (ii)

rubbery inclusions in glassy matrix, and (iii) glassy inclusions in glassy matrix. This choice of three temperatures, in addition to illustrating the ambient and low temperature impact properties of the blend, enables a distinction of impact-toughening mechanisms in the respective states of the blend.

Also presented in this paper are the results of dynamic mechanical measurements on a torsion pendulum in the temperature range  $-100-100^{\circ}\text{C}$ . Correlation of impact strength with the area under the loss peaks occurring below the measuring temperature of impact strength is presented, and the significance of viscoelastic energy dissipation mechanism of toughening in this blend is discussed.

## EXPERIMENTAL

### Specimen Preparation

Isotactic polypropylene (PP), Koylene M-3030 (molding grade, melt flow index 3.0), of Indian Petrochemicals Corp. Ltd., and the block copolymer styrene-*b*-ethylene-co-butylene-*b*-styrene (SEBS), Kraton G-1652, of Shell Chemical Co. were used in this work.

Blends of PP and SEBS, of compositions varying from 5–25 wt % SEBS, were prepared by melt blending in a single-screw extruder Betol BM-1820, at a screw rpm of 40 and temperatures 200, 210, 220, and  $220^{\circ}\text{C}$  of first, second, third zones and the die, respectively. The unblended PP was also processed under identical extrusion conditions to impart it a thermal history similar to the blend samples. Thick strands obtained from extruder were chopped in a granulator, and the granules after washing and drying were injection- or compression- molded into test specimens. Injection molding on a Windsor injection molding machine was done at an injection pressure of  $600\text{ kg/cm}^2$  and injection rate of  $4\text{ cm/s}$ , using a temperature profile of 200, 210, and  $210^{\circ}\text{C}$  of first, second zones, and the nozzle, respectively. Injection-molded specimens of dimensions  $5.5 \times 1.3 \times 0.5\text{ cm}$  with triangular notch of 2.5 mm depth and  $60^{\circ}$  angle were used for impact tests. For dynamic mechanical measurements, test specimens of dimension  $9 \times 1 \times 0.1\text{ cm}$  were cut from compression-molded sheets prepared on a Carver laboratory press at  $180^{\circ}\text{C}$  and  $300\text{ kg/cm}^2$  pressure.

### Measurements

Izod impact strengths of notched samples were measured on a pendulum type impact testing machine (FIE 0.42). Breaking energy calculated from the difference of potential energy of the pendulum striker before and after the impact was used for determination of impact strength (expressed as breaking energy per unit breadth of the specimen<sup>19</sup>, without any further correction for kinetic energy, etc. Hence these values may be emphasized only for their relative magnitudes, as is done in this work. The minimum number of samples tested for each case was five, and the results were quite consistent within 5–8%.

Impact strength was measured at ambient temperature ( $25 \pm 2^\circ\text{C}$ ) and the two low temperatures  $-30$  and  $-190^\circ\text{C}$ . For measurements at low temperatures, samples were kept immersed for at least 2 h in suitable low temperature liquid baths: containing liquid air in the case of  $-190^\circ\text{C}$  and an appropriate mixture<sup>20</sup> of acetone and liquid air in the case of  $-30^\circ\text{C}$ . Samples were transferred to the impact testing machine immediately before testing, and tests were conducted within the shortest possible time, generally a fraction of a minute. During this short time, though the temperature in the interior did not vary owing to low thermal conductivity of polymers, some variation of surface temperature needed to be averted. This was done by continuous pouring of the low-temperature bath liquid over the sample loaded on the machine till the release of impact pendulum.

Dynamic mechanical properties were measured on a torsion pendulum fabricated in the laboratory with a photodyne attachment for recording amplitude and time period of oscillations. Measurements were made in the temperature range  $-100$ – $100^\circ\text{C}$  by using a thermostated chamber surrounding the specimen and a copper–constantan thermocouple placed close to the specimen for measuring the temperature. The total temperature range was covered in more than 10 h from the lowest to the highest temperature, allowing at least 5–10 min for temperature stabilization of the sample at each temperature of measurement. From the time period  $t$  and the logarithmic decrement  $\Lambda$  determined from the recorded amplitude curves, the dissipation factor ( $\tan \delta$ ) and in-phase modulus ( $G'$ ) were calculated by following relations<sup>21</sup>:

$$\tan \delta = \Lambda/\pi$$
$$G' = \frac{64\pi^2 IL}{CD^3 \mu t^2}$$

where  $L$ ,  $C$ , and  $D$  are, respectively, the length, breadth, and thickness of specimen,  $I$  is the moment of inertia of the oscillating system, and  $\mu$  is the shape factor whose value for the rectangular specimen of  $C/D > 2$  is taken as<sup>21</sup>  $\mu = 5.33 (1 - 0.63 D/C)$ .

Scanning electron micrographs of the fracture surfaces of the specimens impact fractured at different temperatures were recorded on a Stereoscan S4-10 (Cambridge Instruments Ltd.) scanning electron microscope.

## RESULTS AND DISCUSSION

### Effect of Temperature on Impact Toughening

Notched Izod impact strengths of PP/SEBS blend at various blend compositions, at the three test temperatures, ambient,  $-30^\circ\text{C}$  and  $-190^\circ\text{C}$  are given in Table I. Variations of impact strength with SEBS content at the three test temperatures are shown in Figure 1. At ambient temperature (Fig. 1), with increasing SEBS content, impact strength increases very slowly until 5% SEBS content and much rapidly beyond that. At 15% SEBS content

TABLE I  
Notched Izod Impact Strength of PP/SEBS Blend at Different Temperatures

SEBS content (wt %)	Impact strength (J/m)		
	Ambient temp	-30°C	-190°C
0	25.7	17.4	17.1
5	30.8	18.8	18.3
10	70.0	23.7	18.4
15	220.0	24.5	19.5
25	Not broken	37.3	21.8

a nearly tenfold increase of impact strength of the parent PP is observed; at higher SEBS content, however, the samples did not break under the applied impact loading conditions. This increase of impact strength is quite comparable to the case of other impact modifiers of PP for example EPDM.<sup>12</sup>

At -30°C (Fig. 1), the impact strength increases very slowly and almost linearly with increasing SEBS content. Increase of impact strength over the studied entire range of blend composition is considerably smaller than the case of ambient temperature. The essential difference in these two cases

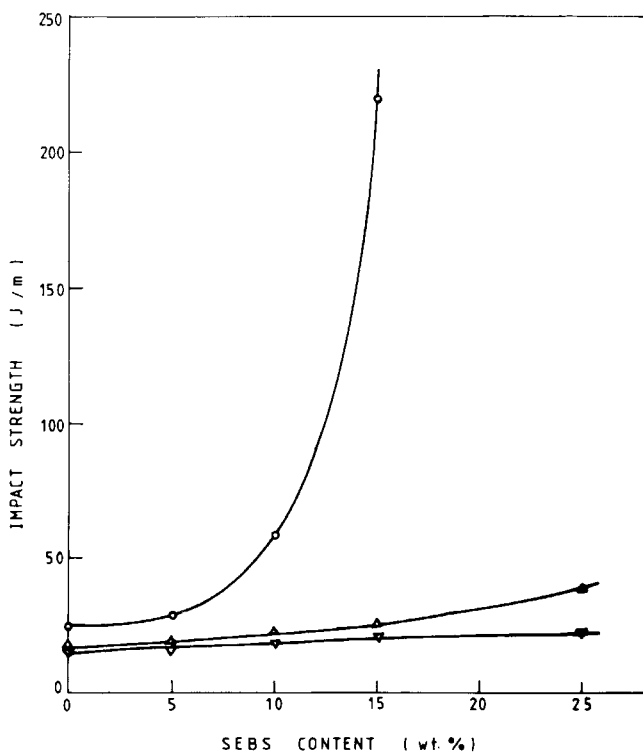


Fig. 1. Variation of impact strength with blend composition of PP/SEBS blend at various temperatures; (○) ambient temperature; (△) -30°C; (▽) -190°C.

is that at  $-30^{\circ}\text{C}$  the matrix PP is in its glassy state while at ambient temperature the matrix is above its glass transition temperature. This might be due to the prevalence of different mechanisms of impact toughening of PP above and below its glass transitions temperature.

At  $-190^{\circ}\text{C}$  (Fig. 1), the impact strength increase is almost negligible in the entire range of blend composition studied. At this temperature, although SEBS is in its glassy state, some effect of the dispersed phase domains is apparent on the impact strength which increases slightly but continuously with increasing SEBS content of the blend. Thus, though glassy nature of the dispersed phase domains produces no significant improvement of toughness, its effect in mode of fracture seems quite significant, as discussed later in this paper.

Variations of impact strength with temperature at constant blend compositions are shown in Figure 2. Owing to a limited number of data points, these curves do not show the usually reported features, such as a two-step increase of impact strength (one at  $T_g$  of the dispersed phase and the other at a higher temperature)<sup>22-24</sup> and/or the maxima in impact strength at temperatures corresponding to the glass transition relaxation peaks in dynamic mechanical loss data.<sup>8,25-28</sup> From these data we may compare the relative increase of impact strength in terms of the temperature coefficient in the two regions as described below. Temperature coefficient of impact strength ( $d\sigma_{\text{impact}}/dT$ ) is calculated as the increase of impact strength ( $\sigma_{\text{impact}}$ ) in the specified temperature range divided by the temperature gap. Values of  $d\sigma_{\text{impact}}/dT$  in the two regions, (a) between  $T_g$  of the dispersed phase (i.e., EB block of SEBS), viz.  $-60^{\circ}\text{C}$  and the  $T_g$  of the matrix, viz.  $0^{\circ}\text{C}$ , and (b) between  $T_g$  of the matrix and the ambient temperature, are shown in Table II with subscripts  $g$  (glassy matrix state) and  $f$  (flexible matrix

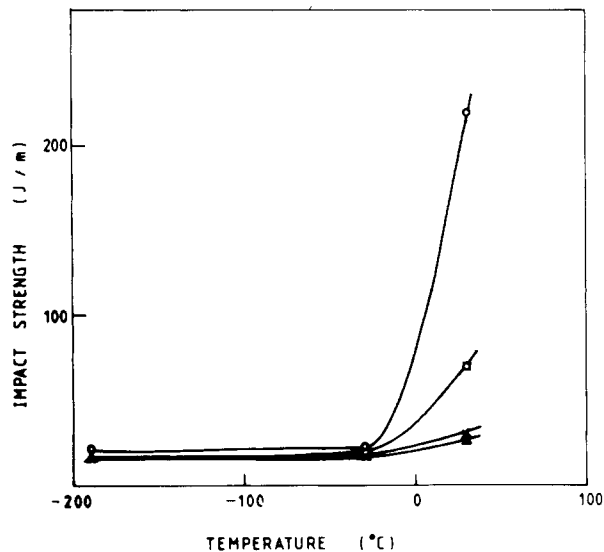


Fig. 2. Variation of impact strength with temperature for PP/SEBS blend at various SEBS contents (%): ( $\Delta$ ) 0; (+) 5; ( $\square$ ) 10; ( $\circ$ ) 15.

TABLE II  
Temperature Coefficients of Impact Strength ( $d\sigma_{\text{impact}}/dT$ ) in "Flexible" and "Glassy"  
Matrix States and Their Ratio

SEBS content (wt %)	$d\sigma_{\text{impact}}/dT$ ( $\text{J m}^{-1} \text{ } ^\circ\text{C}^{-1}$ )		$(d\sigma_{\text{impact}}/dT)_f/(d\sigma_{\text{impact}}/dT)_g$
	Flexible matrix	Glassy matrix	
0	0.20	0.063	3.17
5	0.24	0.075	3.20
10	1.28	0.26	4.92
15	5.60	0.73	7.67

state) for the regions (a) and (b), respectively. This analysis shows that:

1. The temperature coefficient of impact strength increases with increasing SEBS content of the PP/SEBS blend.

2. The temperature coefficient of impact strength is higher in the flexible matrix state than in the glassy matrix state by a factor of 3–8 depending on the elastomer (SEBS) content of the blend.

3. The effect of elastomer content on impact strength improvement is considerably greater in the flexible matrix state than the glassy matrix state.

Similar effects of glassy and flexible matrix states on the impact strength of the blend of PP with EPDM are seen in the results of Yang et al.,<sup>12</sup> where the Charpy impact strength vs. blend composition showed much smaller increase at  $-20$  or  $-40^\circ\text{C}$  than at ambient temperature.

This observed difference of the impact toughening behavior of PP/SEBS blend in glassy and flexible matrix states indicates the predominance of different mechanisms of toughening in the two regions. Previous work<sup>18</sup> on PP/SEBS blend shows the occurrence of shear yielding at ambient temperature and an increase in the work of yield with increasing SEBS content. In the glassy matrix state one would expect suppression of shear yielding, while crazing as toughening mechanism remains operative below  $T_g$  of polymers. This seems supported by the reported<sup>29,30</sup> crazing behavior of PP at different temperatures, where  $-20^\circ\text{C}$  is stated as the limit below which crazes were sufficiently large and above which very small or no crazes were apparent in the fracture surface of PP. Furthermore, a predominance of shear yielding mechanism in flexible matrix state and crazing in glassy matrix state is also stated by Galli, Danesi, and Simonazzi<sup>11</sup> about the impact toughening of the blends of PP with other elastomers.

Considering the prevalence of shear yielding and crazing mechanisms in respectively the flexible and glassy matrix states, and the observed difference of impact behavior of this blend in the respective regions, it may be presumed that shear yielding produces greater impact toughening than crazing. However, though the exact contributions from crazing and shear yielding in PP is not known in PP,<sup>10</sup> the observed difference of impact toughening in flexible and glassy matrix states of this blend seems much greater than normally expected for the above-stated two mechanisms. As discussed later in this paper, a third mechanism, viz. "viscoelastic energy dissipation," may also be operative in the impact toughening of this blend

and its contribution at ambient temperature may be greater owing to the occurrence of the viscoelastic relaxation of the matrix PP below the ambient temperature.

### Dynamic Mechanical Properties

Results of dynamic mechanical measurements on a torsion pendulum at frequency  $\sim 1$  Hz are presented in Figures 3 and 4 as the variations of in-phase shear modulus ( $G'$ ) and loss tangent ( $\tan \delta$ ) with temperature at fixed blend compositions. Two relaxations, showing sharp decrease in modulus and peaks in  $\tan \delta$  at corresponding positions, are apparent in these data. The loss peak around  $10^\circ\text{C}$  represents glass transition relaxation of the major component PP of the blend, as recognized by other authors.<sup>31-35</sup> The other loss peak, situated around  $-70^\circ\text{C}$ , may be attributed to glass transition relaxation of EB block of SEBS elastomer, owing to its closeness with the nearest resembling systems such as polybutadiene<sup>36-38</sup> and polyethylene.<sup>39-41</sup> The two loss peaks representing glass transitions of the individual components of the blend are quite distinct and without any trend of approaching towards each other; this supports the two-phase incompatible character of this blend.

A small lowering of about  $5^\circ\text{C}$  in temperature of loss peak and an increase in peak area or peak height are seen for the glass transition peak of PP in the case of blends with respect to unblended PP, without any detectable

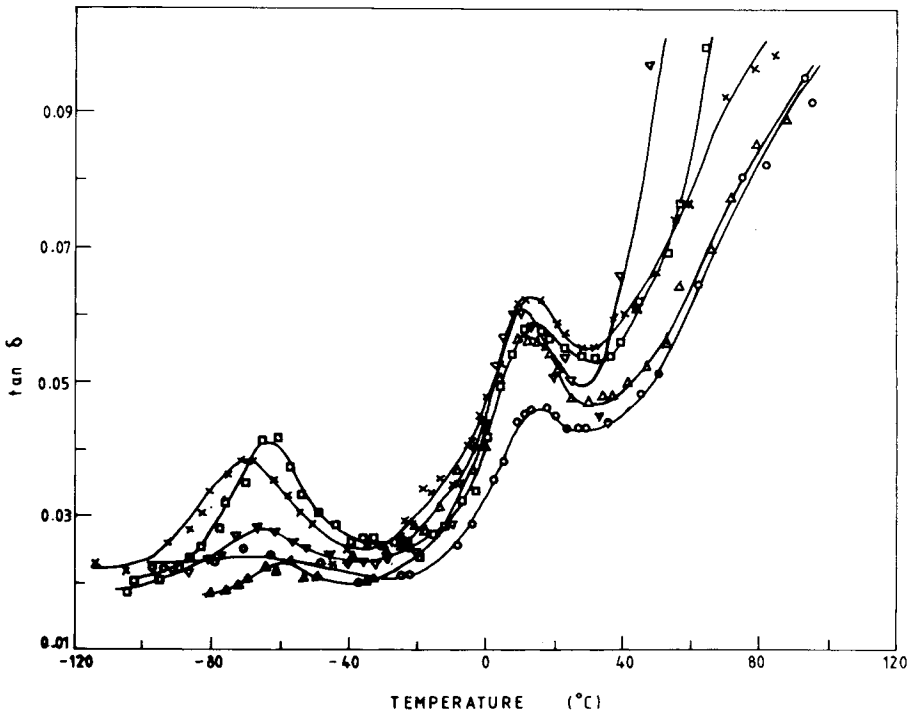


Fig. 3. Variation of in-phase shear modulus ( $G'$ ) with temperature for PP/SEBS blend at various SEBS contents (%): (○) 0; (△) 5; (▽) 10; (+) 15; (□) 20.

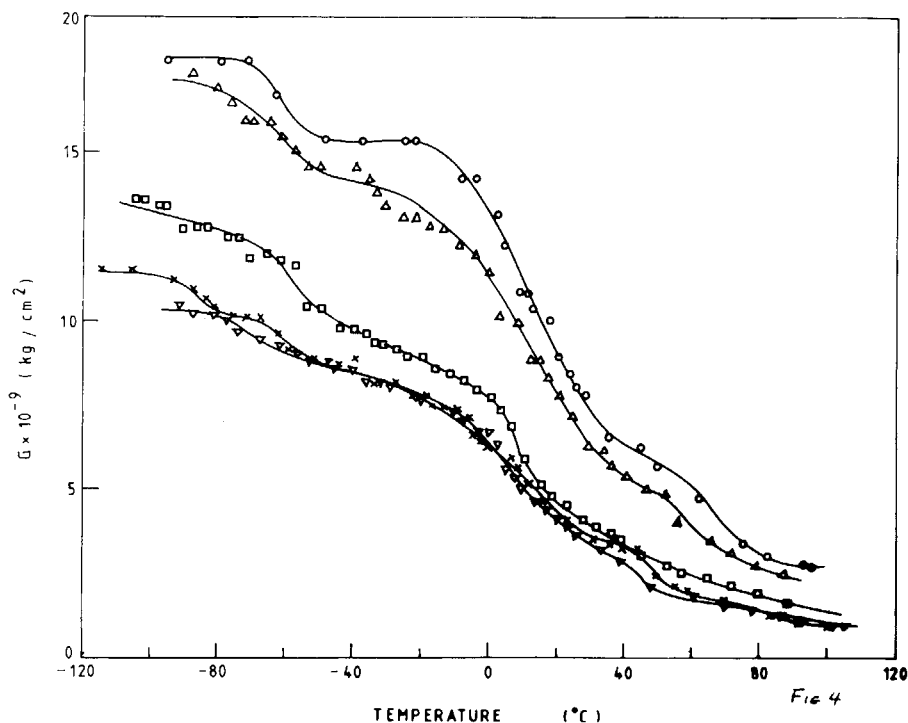


Fig. 4. Variation of dissipation factor ( $\tan \delta$ ) with temperature for PP/SEBS blend at various SEBS contents (%): (○) 0; (△) 5; (▽) 10; (+) 15; (□) 20.

effect of varying SEBS content. This decrease of glass transition temperature of PP is in good qualitative agreement with the previously reported<sup>17</sup> decrease of crystallinity of PP on blending with SEBS. On the other hand, the area and height of the glass transition peak of the elastomer component increase with increasing SEBS content in a manner shown in Figure 5 the increase levelling off at higher SEBS contents. Increase of area and height of elastomer loss peak is known for various other rubber-toughened polymers.<sup>37,38,42</sup> The temperature of the SEBS loss peak varies non linearly with blend composition by about 10°C, showing a minimum around 15% SEBS content (Fig. 5). Bares<sup>43</sup> described the depression in  $T_g$  for dispersed glassy microphases of thermoplastic elastomer to arise from the size of dispersed phase domains as well as the interfacial effects at the domain boundaries. Although an exact correlation of domain size with SEBS content is difficult for this case of irregularly shaped SEBS domains, an indication of continuous increase of average domain size with SEBS content is inherent in the observed<sup>16</sup> continuously increasing abundance of larger domains of SEBS. The observed nonlinear decrease of  $T_g$  is apparently a combined effect of domain size and interfacial effects. Interfacial effects at domain boundaries may not be negligible owing to close proximity of solubility parameter of the EB block of SEBS and PP; solubility parameters 7.90 and 9.07 (cal/cc)<sup>1/2</sup> for EB and PP, respectively.<sup>44</sup>

Shear modulus of PP decreases on blending with elastomer SEBS, like the known<sup>37,45</sup> behavior of other rubber toughened polymers. However, the decrease of  $G'$  is non linear with blend composition in this case, as shown



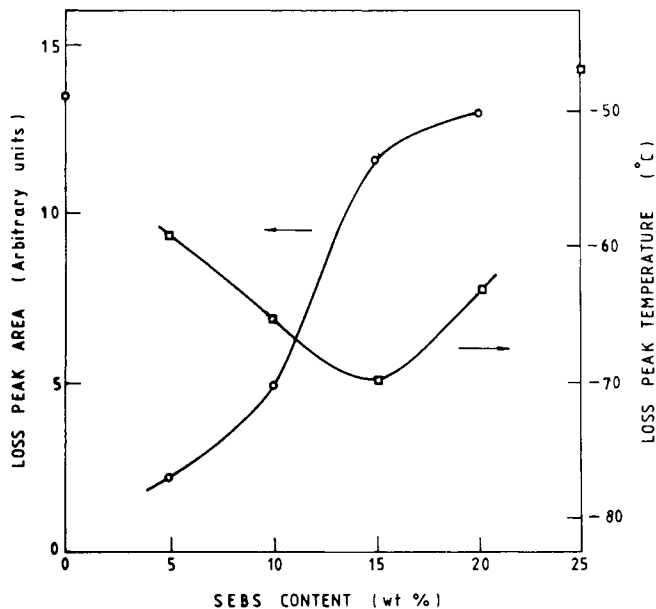


Fig. 5. Variation of area under SEBS loss peak and the peak temperature with SEBS content of the PP/SEBS blend.

in Figure 6. Initially at 0–5% SEBS content  $G'$  shows a very small decrease followed by a rapid decrease in the region 5–10% SEBS content. Thereafter,  $G'$  again increases slightly after passing through a minimum around 10–15% SEBS content. This nonlinearity of variation of shear modulus is apparent at all temperatures (Fig. 6); the features of decrease and increase around the minima becoming sharper with decreasing temperature. This suggests a greater effect of the elastomer component in decrease of shear modulus in the glassy matrix state than the flexible matrix state. Position of minima in  $G'$  remains unchanged with temperature. Minima in  $G'$  of the blend and in  $T_g$  of the elastomer component in the blend occur incidentally at identical blend composition, thus reinforcing the point that rubbery behavior of SEBS in this blend is dominant at blend composition around 15% SEBS content. Furthermore, in previous studies<sup>16,17</sup> on PP/SEBS blend, maxima, minima, or sudden change in properties such as melt viscosity, tensile modulus, and elongation at break were found around the same critical blend composition, viz., 10–15% SEBS content.

### Viscoelastic Energy Dissipation

Although a lot is said in the literature about shear yielding and crazing mechanisms of toughening: one must not ignore the significance of Kausch's statement<sup>46</sup> that any molecular process which promotes distribution and dissipation of energy would enhance impact resistance of polymers. Viscoelastic relaxation of polymers is an important molecular mechanism of energy dissipation. Some authors<sup>8,47</sup> emphasized the importance or need of comparable time scales or frequencies of impact tests (which is generally  $10^2$ – $10^3$  Hz) and of dynamic mechanical measurements (which is generally  $10^0$ – $10^1$  Hz) for the correlation of impact and dynamic mechanical prop-

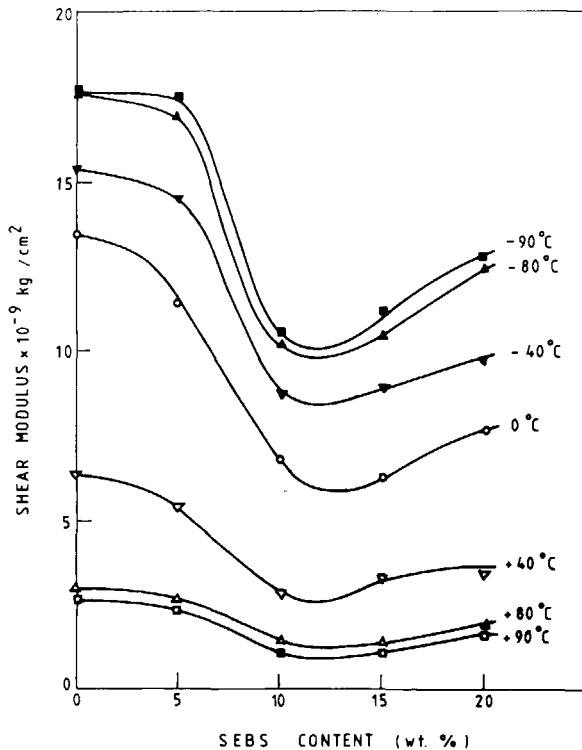


Fig. 6. Variation of dynamic mechanical shear modulus ( $G'$ ) with SEBS content of the PP/SEBS blend at various temperatures.

erties. Various types of correlations between impact strength and dynamic mechanical properties are presented in the literature<sup>8,25-28,38,47-50</sup> such as (i) occurrence of peaks in impact strength at the same temperatures as the loss peaks in  $\tan \delta$ , (ii) linear variations of impact strength with  $\tan \delta$  and in-phase modulus, and/or (iii) correlation between impact strength and area of rubber component's loss peak.

Since viscoelastic relaxations remain frozen at temperatures below the relaxation region, the impact toughness above the relaxation region would be expected higher than that below the relaxation region owing to the contribution of viscoelastic energy dissipation in the impact toughness. Correlation of impact and dynamic mechanical properties in terms of the area of rubber component's loss peak are presented by some authors.<sup>38,50</sup> We consider it more appropriate to include the area of the matrix component's loss peak also in such a correlation, if the viscoelastic relaxation of the loss peak occurs below the impact test temperature. This is the case with the present blend at ambient temperature. Such a correlation for the present data is described below.

A schematic curve of viscoelastic energy dissipation as a function of temperature for a two-phase blend is shown in Figure 7, where loss peaks  $A$  and  $B$  correspond to the relaxations of elastomer and matrix phases, respectively.  $S_A$  and  $S_B$  denote areas under peaks  $A$  and  $B$ , respectively. The temperature regions  $T_1$ ,  $T_2$ , and  $T_3$  indicated in Figure 7 are such that

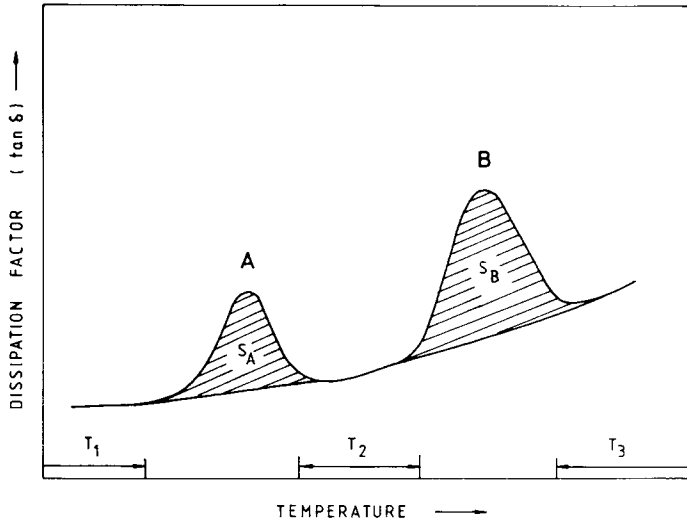


Fig. 7. Schematic representation of viscoelastic energy dissipation curve for a two-phase system showing distinct two relaxations. The three regions of temperature  $T_1$ ,  $T_2$ , and  $T_3$  and the areas  $S_A$  and  $S_B$  are described in the text.

$T_1$  is below both relaxations,  $T_2$  is above relaxation A but below relaxation B, and  $T_3$  is above both the relaxations. The three temperatures of impact tests, viz.  $-190^\circ\text{C}$ ,  $-30^\circ\text{C}$ , and ambient temperature, fall in the regions  $T_1$ ,  $T_2$ , and  $T_3$ , respectively, with respect to the dynamic mechanical loss curve (Fig. 4) for this blend. The observed differences in toughening behavior of this blend at the three temperatures is qualitatively consistent with the viscoelastic energy dissipation of the respective relaxations. The rubber component's loss peak, which is smaller in area, seems to produce a smaller increase (at  $-30^\circ\text{C}$ ) of impact strength than the combined effect of both relaxations (at ambient temperature).

Variations of impact strength with area under experimental loss peaks are shown in Figures 8 and 9. At ambient temperature (Fig. 8), the impact

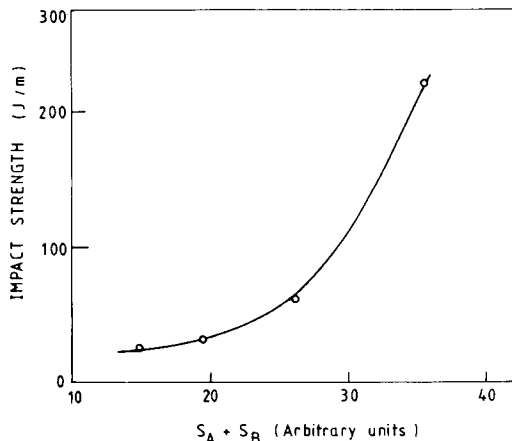


Fig. 8. Variation of impact strength at ambient temperature for PP/SEBS blend with total area under both PP and SEBS loss peaks ( $S_A + S_B$ ).

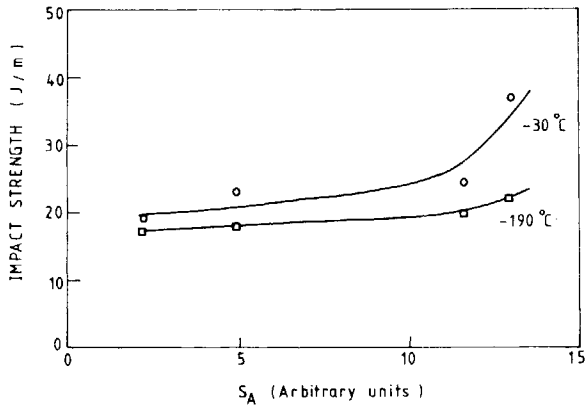


Fig. 9. Variation of low temperature impact strength for PP/SEBS blend with area  $S_A$  under SEBS loss peak.

strength increases with increasing total area ( $S_A + S_B$ ) of both the loss peaks occurring below this temperature. At  $-30^\circ\text{C}$  (Fig. 9), the impact strength increases with increasing area ( $S_A$ ) of the loss peak occurring below this temperature. At  $-190^\circ\text{C}$ , the impact strength does not show any appreciable variation with the area  $S_A$  or  $S_A + S_B$  (one such variation is shown in Fig. 9), which is expected for the frozen state of both the relaxations at this lowest temperature. The nonlinear shape of impact strength vs. loss peak area curve at the two higher temperatures is quite similar to impact strength vs. rubber component's loss peak area curves reported by Keskkula et al.<sup>50</sup> for HIPS. The absence of correlation at  $-190^\circ\text{C}$  and the increase of impact strength with area of viscoelastic relaxation peaks at the other two temperatures indicate the role of viscoelastic energy dissipation mechanism in impact strength enhancement of this blend. The role of viscoelastic energy dissipation mechanism seems further emphasized by the observed difference of impact toughening at ambient temperature and at  $-30^\circ\text{C}$ ; this difference is apparently larger than normally expected for the prevalence of shear yielding or crazing mechanisms at the respective temperatures. At ambient temperature, toughening is predominantly due to shear yielding plus the viscoelastic energy dissipation of both relaxations of matrix component PP and the elastomer, whereas at  $-30^\circ\text{C}$  the toughening is predominantly due to crazing and viscoelastic energy dissipation of the elastomer component's relaxation.

### Scanning Electron Microscopy

Scanning electron micrographs reveal some distinctions in the mode of fracture of PP/SEBS blend at the three temperatures of measurements. Micrographs of impact fractured surfaces at ambient temperature,  $-30^\circ\text{C}$ , and  $-190^\circ\text{C}$  are shown in Figures 10, 11, and 12, respectively. Incorporation of SEBS increases the coarseness of the fracture surface of PP at all the three temperatures.

At ambient temperature (Fig. 10) the increase of coarseness of fracture surface with increasing SEBS content is clearly seen, which arises due to

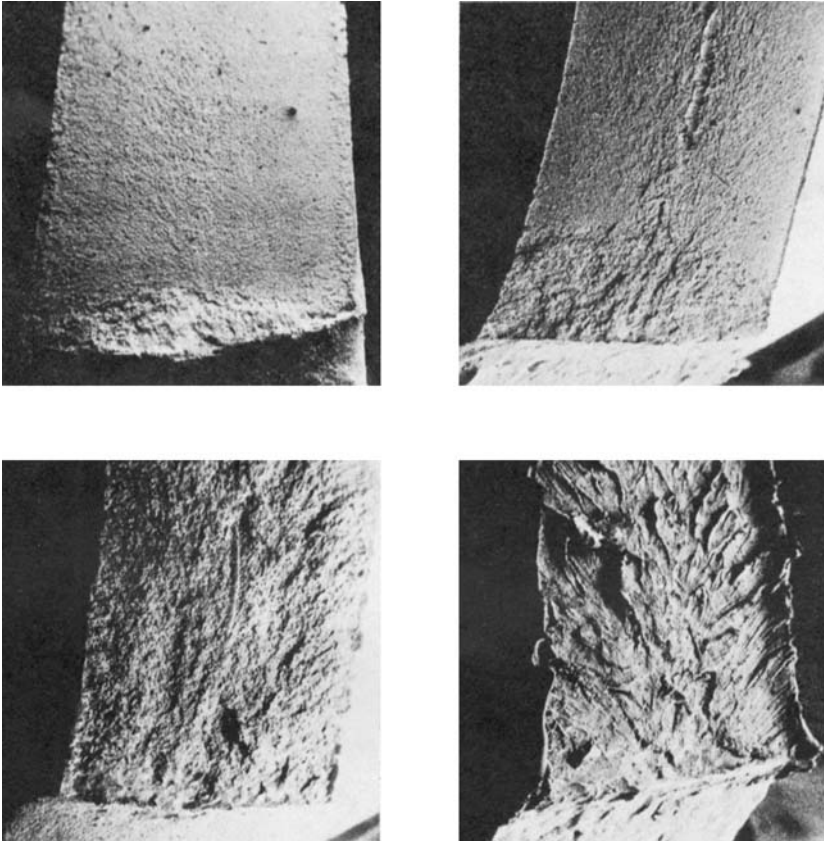


Fig. 10. Scanning electron micrographs of impact fractured surfaces (fractured at ambient temperature) of PP/SEBS blend at various SEBS contents (%): (a) 0; (b) 5; (c) 10; (d) 15.

the effect of dispersed SEBS domains on the propagation of crack during fracture. Features of ductile fracture are clearly seen at 15% SEBS content [Fig. 10(d)], while at the lower SEBS contents such distinct features of ductile fracture are not apparent. As already stated, impact strength at 15% SEBS content at ambient temperature was extremely high, and difficulties in impact failure were encountered at still higher SEBS content. This suggests a transition from brittle to ductile fracture occurring around 15% SEBS content at ambient temperature for PP/SEBS blend.

AT  $-30^{\circ}\text{C}$  the coarseness of fracture surface increases with increasing SEBS content (Fig. 11). Unlike the case of ambient temperature, the features of ductile fracture are not apparent at  $-30^{\circ}\text{C}$  even up to the highest SEBS content (i.e., 25%), presumably owing to the glassy state of the matrix PP. Impact strength improvement up to the highest SEBS content in this case is also not so high as in case of ambient temperature. A comparison of these results for say 15% SEBS content at ambient temperature and  $-30^{\circ}\text{C}$  [Fig. 10(d) and 11(c)] suggests the possibility of determining from further experiments a temperature of transition from brittle to ductile fracture for this blend; this transition temperature would be somewhere between  $-30^{\circ}\text{C}$  and

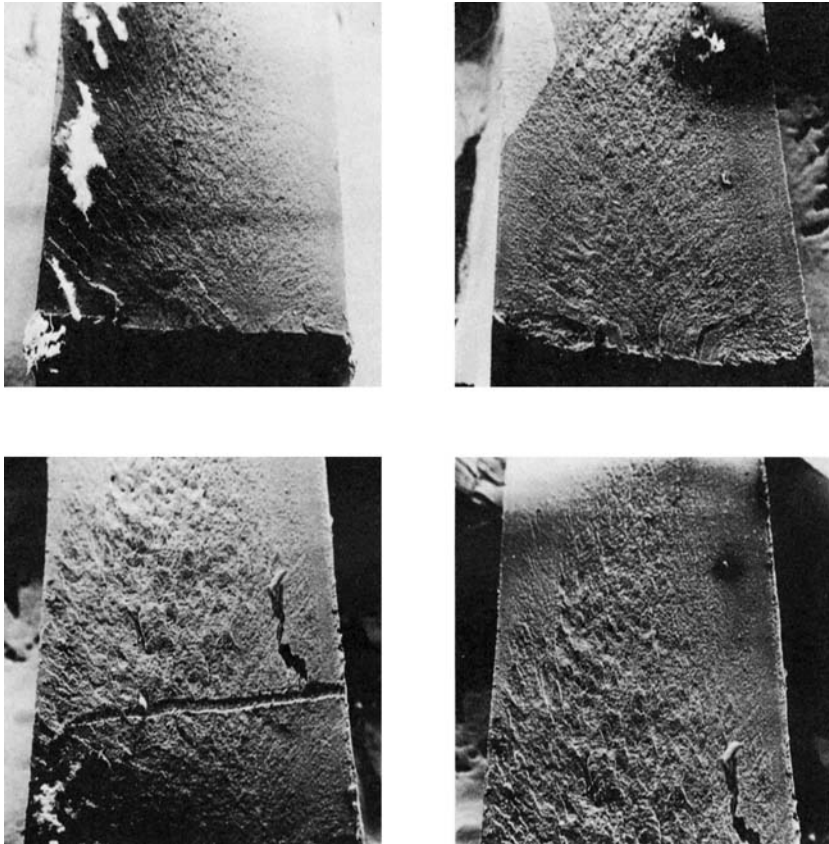


Fig. 11. Scanning electron micrographs of impact fractured surfaces (fractured at  $-30^{\circ}\text{C}$ ) of PP/SEBS blend at various SEBS contents (%): (a) 5; (b) 10; (c) 15; (d) 25.

ambient temperature. Such a transition for a PP/EPM is known to occur around  $-10-0^{\circ}\text{C}$ .<sup>11</sup>

At the lowest temperature  $-190^{\circ}\text{C}$  (Fig. 12) the fracture surface of the blend is distinctly different from those at the other two temperatures. Features of brittle catastrophic failure and shattering of the specimen into fragments are seen at this lowest temperature for all the compositions of the blend. Crazes are also visible as parallel striations propagating quite long distances in certain regions of the fracture surfaces [Fig. 12 (b),(c),(d)] of the blend. Comparison of the fracture surfaces of unblended PP [Fig. 12(a)] with that of the blend [Figures 12(b),(c),(d)] shows the role of glassy SEBS domains in generating this highly brittle character of fracture at  $-190^{\circ}\text{C}$ .

In addition to the glassy nature of the dispersed phase domains, there is a possibility of greater gap at the interphase boundary due to the difference of volume contraction of the two phases at this lowest temperature than at the other two temperatures. Hence the observed role of SEBS in enhancing the brittleness of the fracture may be a combined effect of both of these.

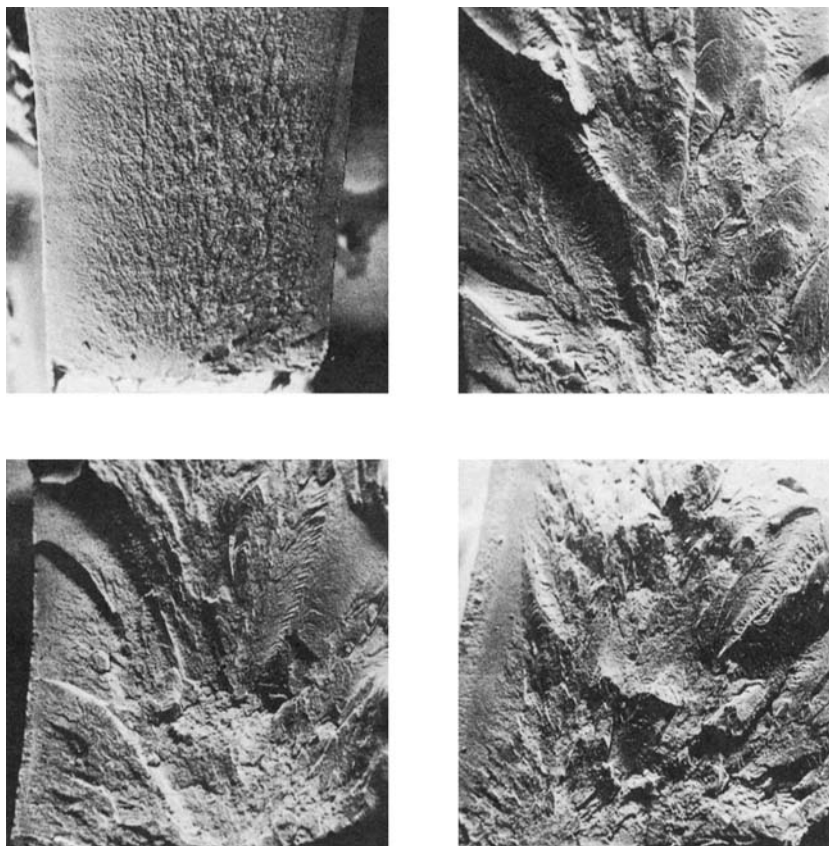


Fig. 12. Scanning electron micrographs of impact fractured surfaces (fractured at  $-190^{\circ}\text{C}$ ) of PP/SEBS blend at various SEBS contents: (a) 0; (b) 5; (c) 10; (d) 15.

## CONCLUSION

Impact toughness of PP is greatly enhanced on blending with SEBS, depending on SEBS content and temperature. At ambient temperature, a 15% SEBS incorporation produces about a tenfold increase in the impact strength of PP, whereas at  $-30^{\circ}\text{C}$  the increase is only about twofold at the same SEBS content. At  $-190^{\circ}\text{C}$ , where the dispersed phase is in glassy state, there is no appreciable improvement of impact strength.

Dynamic mechanical properties show the two-phase incompatible blend character of this blend and a nonlinear decrease of in-phase modulus with SEBS content, showing minima around 10–15% SEBS content. Correlation of impact strength at given temperature with the area under dynamic mechanical loss peaks occurring below that temperature suggests the significance of viscoelastic energy dissipation in the impact toughening of this blend.

The observed large difference of toughening at ambient temperature and at  $-30^{\circ}\text{C}$  seems to arise from the relative contributions from the three mechanisms of toughening, viz., shear yielding, crazing, and viscoelastic

energy dissipation. At ambient temperature, toughening is predominantly due to shear yielding plus viscoelastic energy dissipation of both relaxations of matrix component PP and the elastomer. At  $-30^{\circ}\text{C}$ , the toughening is predominantly due to crazing and viscoelastic energy dissipation of only elastomer component's relaxation.

A transition from brittle to ductile mode of fracture at ambient temperature occurs at blend composition around 15% SEBS content. No such transition is observed at the other two lower temperatures over the entire range of the blend composition studied.

### References

1. D. R. Paul and S. Newman, *Polymer Blends*, Academic, New York, 1972, Vol. 2.
2. W. M. Speri and G. R. Patrick, *Polym. Eng. Sci.*, **15**, 668 (1975).
3. R. C. Thamm, *Rubber Chem. Technol.*, **50**, 24 (1977).
4. E. Martuscelli, *Polym. Eng. Sci.*, **24**, 563 (1984).
5. S. Danesi and R. S. Porter, *Polymer*, **19**, 448 (1978).
6. M. Kakugo and H. Sadanori, *Sumitomo Kagaku Tokushugo*, **1**, 22 (1979).
7. J. Karger-Kocsis, A. Kallo, A. Szafner, G. Bodor, and Z. Senyei, *Polymer*, **20**, 37 (1979).
8. J. Karger-Kocsis and V. N. Kuleznev, *Polymer*, **23**, 699 (1982).
9. F. C. Stehling, T. Huff, C. S. Speed, and G. Wissler, *J. Appl. Polym. Sci.*, **26**, 2693 (1981).
10. P. L. Fernando and J. G. Williams, *Polym. Eng. Sci.*, **21**, 1003 (1981).
11. P. Galli, S. Danesi, and T. Simonazzi, *Polym. Eng. Sci.*, **24**, 544 (1984).
12. D. Yang, B. Zhang, Y. Yang, Z. Fang, G. Sun, and Z. Feng, *Polym. Sci. Eng.*, **24**, 612 (1984).
13. A. F. Halasa, D. W. Carlson, and J. E. Hall, U.S. Pat. 4,226,952 (1980).
14. G. G. A. Bohn, C. R. Hamed, and L. E. Yescelius, *Ger. Offen.* 2,885,697 (1978).
15. C. Markin and H. L. William, *J. Appl. Polym. Sci.*, **25**, 2451 (1980).
16. A. K. Gupta and S. N. Purwar, *J. Appl. Polym. Sci.*, **29**, 1079 (1984).
17. A. K. Gupta and S. N. Purwar, *J. Appl. Polym. Sci.*, **29**, 1595 (1984).
18. A. K. Gupta and S. N. Purwar, *J. Appl. Polym. Sci.*, **29**, 3513 (1984).
19. F. Rodriguez, *Principles of Polymer Systems*, McGraw-Hill, New York, 1970, p. 227.
20. *CRC Handbook of Chemistry and Physics*, 63rd ed., CRC Press, Boca Raton, FL, 1982-1983, p. D-224.
21. L. E. Nielsen, *Mechanical Properties of Polymers and Composites*, Vol. I, Marcel Dekker, New York, 1974, p. 49.
22. C. B. Bucknall and D. G. Steet, *SCI Monograph No. 26*, 272 (1967).
23. J. Mann and G. R. Williamson, in *The Physics of Glassy Polymers*, R. N. Haward, Ed., Applied Science, London, 1973, p. 454.
24. C. B. Bucknall, *Toughened Plastics*, Applied Science, London, 1977, Chap. 7.
25. P. I. Vincent, *Polymer*, **15**, 111 (1974).
26. E. J. Sacher *J. Appl. Polym. Sci.*, **19**, 1421 (1975).
27. M. Kisbenyi, M. W. Birch, J. M. Hodgkinson, and J. G. Williams, *Polymer*, **20**, 1289 (1979).
28. J. G. Williams, *Fracture Mechanics of Polymers*, Ellis Harwood, Chichester, 1984, p. 259.
29. H. G. Olf and A. Peterlin, *Polymer*, **14**, 78 (1973).
30. H. G. Olf and A. Peterlin, *J. Polym. Sci., Polym. Phys. Ed.*, **12**, 2209 (1974).
31. H. A. Flocke, *Kolloid Z.*, **180**, 118 (1962).
32. N. G. McCrum, *Polym. Lett.*, **2**, 495 (1964).
33. E. Passaglia and G. M. Martin, *J. Res. Natl. Bur. Std.*, **68**, 519 (1964).
34. A. P. Plochocki, *Kolloid Z. Z. Polym.*, **208**, 168 (1966).
35. A. K. Gupta, V. B. Gupta, R. H. Peters, W. G. Harland, and J. P. Berry, *J. Appl. Polym. Sci.*, **27**, 4669 (1982).
36. T. Miyamoto, K. Kodama, and K. Shibayama, *J. Polym. Sci. A-2*, **8**, 2095 (1970).
37. G. Cigna, *J. Appl. Polym. Sci.*, **14**, 1781 (1970).
38. E. R. Wagner and L. M. Robeson, *Rubber Chem. Technol.*, **43**, 1129 (1970).



39. A. V. Tobolesky, D. W. Carlson, and N. Indicator, *J. Polym. Sci.*, **54**, 175 (1961).
40. R. F. Boyer, *Rubber Rev.*, **34**, 1303 (1963).
41. H. G. Elias, *Macromolecules*, Vol. 1, Plenum, New York, 1977, p. 409.
42. S. Krause and L. J. Broutman, *J. Appl. Polym. Sci.*, **18**, 2945 (1974).
43. J. Bares, *Macromolecules*, **8**, 244 (1975).
44. D. L. Siegfried, D. A. Thomas, and L. H. Sperling, *J. Appl. Polym. Sci.*, **26**, 177 (1981).
45. J. A. Schmitt and H. Keskkula, *J. Appl. Polym. Sci.*, **8**, 132 (1960).
46. H. H. Kausch, *Polymer Fracture*, Springer-Verlag, Berlin, 1978, p. 210.
47. E. Sacher, *J. Macromol. Sci. Phys.*, **B9**, 167 (1974).
48. Y. Wada and T. Kashahara, *J. Appl. Polym. Sci.*, **11**, 1661 (1967).
49. J. Heijboer, *J. Polym. Sci. C*, **16**, 3755 (1968).
50. H. Keskkula, S. G. Turley, and R. F. Boyer, *J. Appl. Polym. Sci.*, **15**, 351 (1971).

Received March 28, 1985

Accepted May 22, 1985